



	Experiment title: Quantitative diffraction on single nano-structures for mechanical, photonic and electronic applications	Experiment number: HS-4670
Beamline: ID01	Date of experiment: from: 26 Jun 2013 to: 02 Jul 2013	Date of report: 3 September 2015
Shifts: 18	Local contact(s): P. Boesecke	<i>Received at ESRF:</i>

Names and affiliations of applicants (* indicates experimentalists):

T.W. Cornelius*, **Z. Ren***, **F. Mastropietro***, **M.-I. Richard**, **S. Labat**, **O. Thomas***, *Im2np (UMR 7334) CNRS, Aix-Marseille University, 13397 Marseille, France*

S. Langlais*, **M. Dupraz***, **G. Beutier***, **M. Verdier***, **M. de Boissieu**, *SIMaP, Grenoble University, Grenoble, France*

V. Favre-Nicolin, *CEA Grenoble, INAC SP2M, Grenoble, France*

J. Eymery, *CEA Grenoble - INAC SP2M/NPSC, Grenoble, France*

Report:

Within the framework of the project ANR MecaniX and the long-term proposal at ESRF we developed a new atomic force microscope for *in situ* studies of the mechanical properties of nanostructures in combination with nanofocused X-ray diffraction. The new tool consists of two stacks of piezo stages facilitating the separate alignment of the sample and the AFM-tip with respect to each other as well to the focused X-ray beam. For reasons of compactness an Akiyama probe is used as AFM force sensor. This new device was installed on the diffractometer at the ID01 beamline (see Fig. 1) which allows for rotating the complete AFM into Bragg condition while keeping the AFM-tip vertical with respect to the sample surface. During this experiment, the X-ray beam was monochromatized either to 8.97 or to 9 keV using the double-bounce channel-cut Si111 monochromator. By means of a tungsten Fresnel zone plate (FZP) with a diameter of 300 μm and an outer zone width of 80 nm, the monochromatic beam was focused down to 400 nm vertically and 900 nm horizontally. The diffracted X-ray beam was recorded either by a two-dimensional MAXIPIX pixel detector with a pixel size of 55 μm x 55 μm or a point detector – an avalanche photo diode (APD). Both detectors were mounted 1.27 m distant from the sample position.

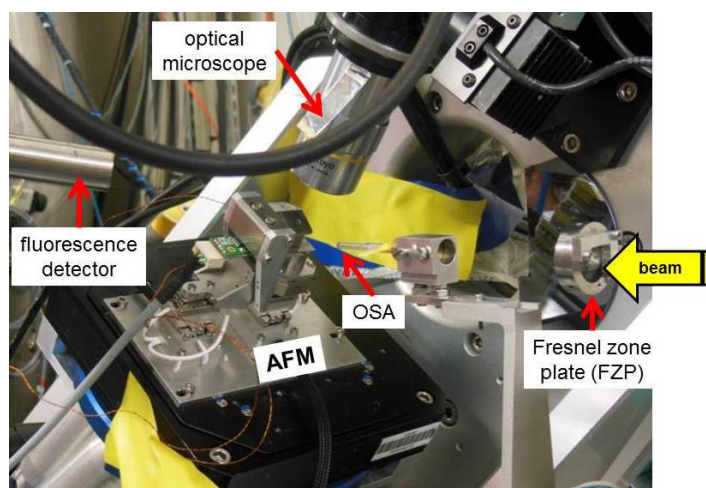


Fig. 1: Photograph of the *in situ* AFM being installed on the diffractometer at the ID01 beamline.

The noise level of the *in situ* AFM installed on the diffractometer at ID01 is in the range of +/- 15 nm while it amounts only to +/- 5 nm mounted on a marble table. This increase in noise is caused by the comparatively harsh conditions compared to a standard AFM lab. The new tool allows for imaging the sample topography, crystallinity, and elemental distribution simultaneously by scanning the AFM-tip and the focused X-ray beam across the sample and recording an AFM image, a scanning X-ray diffraction map (SXDM), and a fluorescence map at the same time. Figures 2 (a), (b), and (c) display the *in situ* images of the sample topography, the Cu-K α fluorescence map, and the SXDM of the Cu111 Bragg reflection for copper nanowires with a diameter of 250 nm on a Si substrate, respectively. Here, the energy of the incident X-rays was 9 keV

surpassing the Cu K-edge and, thus, exciting the Cu- K_{α} fluorescence when illuminating the Cu nanowire. The fluorescence was detected with a ROENTEC energy dispersive detector. The diffracted X-rays were detected by an APD which was directly read out by the AFM controllers. The good agreement of the AFM image and the fluorescence map demonstrate a perfect alignment of the AFM-tip with respect to the focused X-ray beam. However, in the SXDM only a small part of the nanowire fulfills the Bragg condition. This *in situ* mapping was then repeated at 4 different rocking angles within 1° . The different colors in the SXDM displayed in Fig. 2 (d) represent the diffraction signal recorded at the different rocking angles. While rocking the sample by 1° the diffraction signal moves by about $5 \mu\text{m}$ along the nanowire indicating a distortion of the wire.

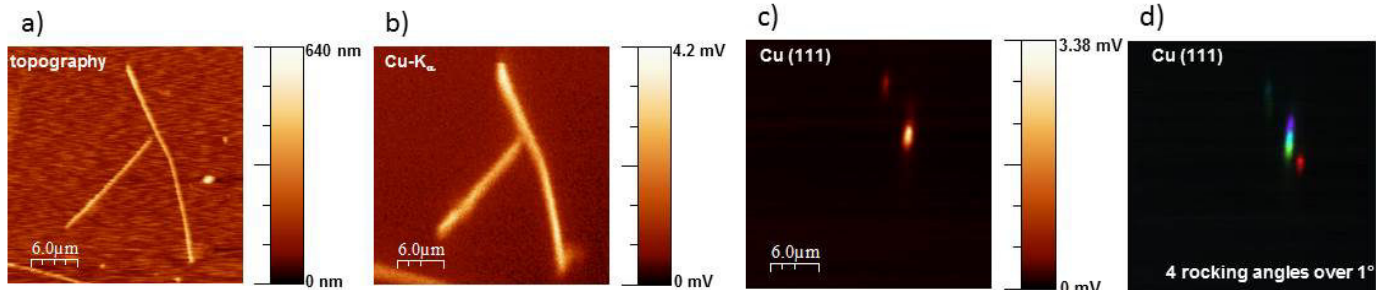
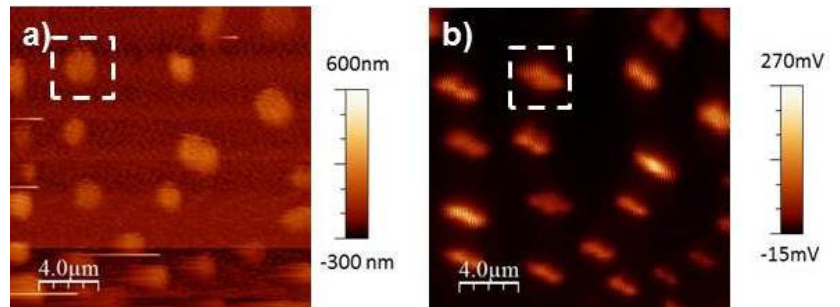


Fig. 2: a) AFM topography, b) Cu- K_{α} fluorescence map, and c) scanning X-ray diffraction map of the Cu111 Bragg reflection for copper nanowires on a Si substrate. d) SXDMs of the Cu111 Bragg peak recorded at 4 different rocking angles. The different colors correspond to the different rocking angles.

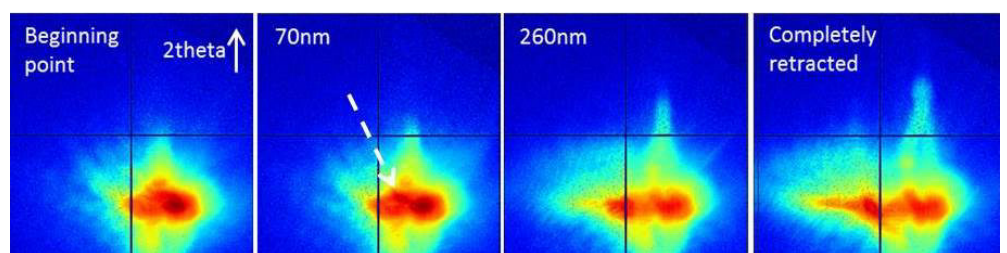
Figures 3 (a) and (b) present the *in situ* AFM image, respectively, the *in situ* SXDM for Au islands grown on a sapphire substrate. These images were taken at the Au(222) Bragg peak at a Bragg angle of 35° employing an X-ray energy of 8.97 keV. The elongated shape of the islands signal in the beam direction in the SXDM originates from the convolution of the island shape and the footprint of the X-ray beam.

Fig. 3: a) *In situ* AFM image and b) *in situ* scanning X-ray diffraction map of Au islands grown on a sapphire substrate. The images were taken at the Au(222) Bragg reflection at $\theta = 35^{\circ}$.



After selecting one of the Au islands which is marked by a dashed square in Fig. 3, an *in situ* indentation test was performed. For this purpose, the AFM-tip was positioned above the selected island, the feedback loop was switched off, and the nano-object was indented using the AFM-tip. Here, the tip was lowered in steps of 10 nm up to a total movement of 260 nm. Subsequently, it was raised likewise until the initial position was reached, and, finally, it was retracted by $5 \mu\text{m}$. At each step a 2D X-ray diffraction image was recorded employing the MAXIPIX detector. A sequence of *in situ* diffraction patterns are displayed in Fig. 4. The initial diffraction pattern when the AFM-tip is just above the top facet of the island is displayed in the image on the left hand side. The first change in the diffraction pattern being highlighted by a dashed arrow in the second image was observed after lowering the AFM-tip by 70 nm. When lowering the AFM-tip further and, thus, indenting the tip further into the Au crystal, the diffraction signal develops an inner structure and a streak along the 2-theta direction appears. A splitting of the diffraction peak and a further elongation along 2-theta is observed during the indentation process. After retracting the tip completely, the diffraction pattern did not return to its initial shape evidencing a plastic deformation of the island.

Fig 4: Sequence of *in situ* X-ray diffraction patterns recorded during the indentation process of an Au island.



For the time being, the force applied on a structure by means of the AFM-tip cannot be directly inferred. Within a first approximation the force can be estimated assuming that the complete movement in z-direction goes into the deflection of the cantilever which has a stiffness of $k = 5 \text{ N/m}$ (according to the provider).